Membrane-bound form of monocyte chemoattractant protein-1 enhances antitumor effects of suicide gene therapy in a model of hepatocellular carcinoma

doi: 10.1038/cgt.2012.3

Membrane-bound form of monocyte chemoattractant protein-1 enhances antitumor effects of suicide gene therapy in a model of hepatocellular carcinoma

Yohei Marukawa,[1] Yasunari Nakamoto,[1] Kaheita Kakinoki,[1] Tomoya Tsuchiyama,[1] Noriho Iida,[1] Takashi Kagaya,[1] Yoshio Sakai,[1] Makoto Naito[3], Naofumi Mukaida,[2] and Shuichi Kaneko[1]

[1]Disease Control and Homeostasis, Graduate School of Medical Science , [2]Division of Molecular Bioregulation, Cancer Research Institute, Kanazawa University, Kanazawa, Japan; and [3]Division of Cellular and Molecular Pathology, Niigata University Graduate School of Medicine, Niigata, Japan

Running title:

ANTITUMOR EFFECTS OF MEMBRANE-BOUND FORM OF MCP-1

Address correspondence and reprint requests to: Dr Shuichi Kaneko, M.D., PhD., Disease control and Homeostasis, Graduate School of Medical Science, Kanazawa University, 13-1 Takara-machi, Kanazawa 920-8641, Japan

Phone: +81-76-265-2231, Fax: +81-76-234-4250, E-mail: skaneko@m-kanazawa.jp

Abstract

Suicide gene therapy using the herpes simplex virus thymidine kinase/ganciclovir (HSV-tk/GCV) system combined with monocyte chemoattractant protein-1 (MCP-1) provides significant antitumor efficacy. The current study was designed to evaluate the antitumor immunity of a newly developed membrane-bound form of MCP-1 (mMCP-1) in an immunocompetent mouse model of hepatocellular carcinoma (HCC). A recombinant adenovirus vector (rAd) harboring the human *MCP-1* gene and the membrane-spanning domain of the *CX3CL1* gene was used. Large amounts of MCP-1 protein were expressed and accumulated on the tumor cell surface. The growth of subcutaneous tumors was markedly suppressed when tumors were treated with mMCP-1, as compared to soluble MCP-1, in combination with the HSV-tk/GCV system (P <0.01). The numbers of Mac-1-, CD4- and CD8a-positive cells were significantly higher in tumor tissues (P <0.05), and tumor necrosis factor (TNF) mRNA expression levels with mMCP-1 were almost 5-fold higher than those with soluble MCP-1. These results indicate that the delivery of the *mMCP-1* gene greatly enhanced antitumor effects following the apoptotic stimuli by promoting the recruitment and activation of macrophages and T lymphocytes, suggesting a novel strategy of immune-based gene therapy in the treatment of patients with HCC.

Keywords

Monocyte chemoattractant protein-1; Herpes simplex virus thymidine kinase; Hepatocellular carcinoma; Membrane-bound form; Monocyte/Macrophages

Introduction

In spite of the recent development of locoregional treatments for hepatocellular carcinoma (HCC), the frequency of tumor recurrence remains high, probably because of insufficient therapeutic effects and the multicentric development of HCC in cirrhotic liver (1-3). Non-surgical treatments of HCC, such as radiofrequency ablation, transcatheter arterial embolization, and transcatheter arterial chemotherapy induce apoptosis of HCC cells, but these treatments do not enhance antitumoral immunity sufficiently. Thus, gene therapy aimed at enhancing antitumor immune responses may be a promising approach to prevent HCC recurrence, when it is combined with non-surgical maneuvers.

We previously reported that monocyte chemoattractant protein-1 (*MCP-1*) gene delivery using recombinant adenovirus vector (rAd) in vivo can enhance the efficacy of suicide gene therapy consisting of the delivery of rAd containing herpes simplex virus thymidine kinase (HSV-tk) and ganciclovir in models of HCC (4, 5) and colon cancer (6). We further demonstrated that the antitumor effects depended on the activation of macrophages (4, 5). The adenovirus-specific spatial and temporal expression pattern may result in the production of the transgene for a limited time (7). Mirroring these characteristics, the adenovirus vector-mediated delivery of *MCP-1* gene alone was not sufficient to reduce tumor growth (5). In order to circumvent this bottleneck, sustained expression of MCP-1 at the tumor site may be required to enhance the efficacy of the gene therapy using *MCP-1* gene.

Systemic or local administration of cytokines has been used to enhance the antitumor immune response induced by many cancer vaccines. However, the systemic

administration of cytokines resulted in unwanted side effects. Recently, tumor therapy that uses a membrane-bound form of cytokine was developed to reduce the side-effects of cytokine in the systemic circulation. These experiments revealed that the membrane-bound form of cytokine not only reduced the side-effects but enhanced the anti-tumor effects by prolonging the half-life of cytokines in the tumor microenvironment (8).

These observations prompted us to design the adenovirus vector driving the expression of membrane-bound form of MCP-1 (mMCP-1) and to evaluate its antitumor effects in a model of HCC. We demonstrated that the delivery of *mMCP-1* gene markedly augmented HSV-tk/GCV suicide gene therapy, compared to that of the soluble MCP-1 (sMCP-1).

Materials and Methods

Recombinant adenovirus vectors

Ad-mMCP1 (Fig. 1a) harboring the human *MCP-1* gene and the membrane-spanning domain of the *CX3CL1* gene driven by the human cytomegalovirus immediate early promoter/enhancer (CMV IE) promoter was prepared, purified, and titrated according to the protocols supplied by the manufacturer (Takara, Tokyo, Japan). The human MCP-1/CX3CL1 (Fractalkine) chimera was designed as follows. DNA encoding a fragment of human CX3CL1 spanning the intracellular, transmembrane and partial extracellular region was amplified from the full-length CX3CL1 cDNA by PCR with the following primers (5'-GCGAGCTCGGGTACCTTCGAGAAGCAGATCG and 5'-GCGAATTCAGATTGTCACACGGGCACAGG). *SacI*, *KpnI* and *EcoRI* restriction enzyme sites were added at the 5' and 3' ends of this fragment. MCP-1 was also amplified by PCR with the following primers (5'-GCGAGCTCGCCAGCATGAAAGTCTCTGCCG and 5'-GCGGTACCAGTCTTCGGAGTTTGGGTTTGC). *SacI* and *KpnI* restriction enzyme sites were added at the 5' and 3' ends of this fragment. The CX3CL1 and MCP-1 DNA fragments were digested with restriction enzymes by coligation into the *SacI* and *EcoRI* sites of pSTBlue-1 (Novagen, Darmstadt, Germany), generating pSTBlue-1-mMCP1. Then, pSTBlue-1-mMCP1 was digested by *NotI* and *BamHI* restriction enzymes, and the fragment was inserted into the pShuttle Vector (Clontech Laboratories, Mountain View, CA) under the control of CMV IE promoter, generating pShuttle-mMCP-1. pShuttle-mMCP-1 was digested with *PI-SceI*/*I-CeuI* (New England Biolabs. Hitchin, UK), and the purified product was ligated with Adeno-X genome

DNA, containing nearly the full length of the adenovirus type 5 genome lacking the E1 and E3 regions, to generate pAd.mMCP1. Subsequently, Ad-mMCP1 was generated by transfecting 293 cells with pAd.mMCP1, which was linearized with PacI, as described in the manual. Ad-sMCP1 (which expresses sMCP1), Ad-lacZ (which expresses beta-galactosidase (lacZ)) and Ad-tk (which expresses HSV-tk) were constructed as previously described and propagated in 293 cells (Fig. 1b, c, d) (9). The rAds were purified on a cesium gradient, and the titer of rAd was determined by the 50% tissue culture infectious dose ($TCID_{50}$) method (10).

Cell lines and culture

The mouse HCC cell lines (BNL 1NG A2, BNL 1ME A.7R.1, MM45T.Li and Hepa 1-6) and the colon cancer cell line Colon 26 were used in these experiments. Cells were cultured in Dulbecco's modified Eagle medium (DMEM) (Gibco, Long Island, NY) supplemented with 10% heat-inactivated fetal bovine serum (FBS) (Gibco).

Enzyme-linked immunosorbent assay (ELISA) for MCP-1

Aliquots of 1×10^5 HCC lines (BNL 1NG A2, BNL 1ME A.7R.1, MM45T.Li and Hepa 1-6) and the colon cancer cell line, Colon 26 clone 20, were seeded in 1.0 ml of culture media in a 6-well tissue culture plate. After 24 hours, the cells were infected with Ad-mMCP1, Ad-sMCP1 and Ad-lacZ at various multiplicities of infection (MOI). After 48 hours, the cells were harvested and sonicated to obtain the membrane fractions, and the media was collected from each well. Tumor tissues were resected on day 1 after s.c. injection of 5×10^6 MM45T.Li cells infected with indicated rAds (MOI 50) as described below. Tumor tissues were washed with PBS and sonicated to obtain the

membrane fractions. The concentration of MCP-1 was determined by ELISA as described previously (11). Briefly, each well of a 96-well microtiter plate was coated with monoclonal anti-human MCP-1 antibody (ME61; 1 mg/ml) overnight at 41^{o}C. After washing, the plates were blocked by incubation with PBS containing 1% bovine serum albumin (BSA) for 1 hour at 37^{o}C. Diluted sample media was added, and the plate was then incubated for 2 hours at 37^{o}C. Following incubation, the plates were washed and incubated with rabbit anti-MCP-1 antibody (1 mg/ml), followed by alkaline phosphatase-conjugated goat anti-rabbit antibody (1/12,000, Tago, Burlingame, CA), each for 2 hours at 37^{o}C. After the plate was washed, aliquots of 1 mg/ml p-nitrophenylphosphate (Sigma, St Louis, MO) in 1M diethanolamine (Sigma) (pH 9.8) supplemented with 0.5 mM $MgCl_2$ were added to the wells, and the plate was incubated for 40 minutes at room temperature. After the addition of 1M NaOH, the optical density (405 nm wavelength-OD405) was assessed by using an ELISA plate reader (MTP-120; Corona Electric, Ibaragi, Japan).

In vitro chemotaxis assay

In vitro migration assays were performed with the QCM chemotaxis cell migration assay (5 μm, Chemicon International, Temecula, CA) according to the manufacturer's instructions. Briefly, 7.5×10^4 splenocytes were resuspended in 100 μl of RPMI1640 containing 5% BSA and loaded into the upper well of a transwell chamber. The lower wells were filled with 150 μl of supernatant from MM45T.Li cells that were harvested 48 hours after infection with rAds. The cells were incubated for 4 hours at 37^{o}C in a humidified, 5% CO_2 atmosphere. The migrated cells were lysed and detected by the CyQuant GR dye (Molecular Probes, Eugene, OR), and fluorescence was read at an

excitation wavelength of 490 nm and an emission wavelength of 520 nm in a fluorescence microplate reader (Thermo Scientific Fluoroskan Ascent FL, Thermo Fisher Scientific Oy, Vantaa, Finland).

In vitro proliferation assay

In vitro proliferation assays were performed with the CellTiter 96 Aqueous Non-Radioactive Cell Proliferation Assay (Promega, Madison, WI, USA) according to the manufacturer's instructions. Briefly, aliquots of 1×10^4 MM45T.Li cells that were harvested 24 hours after infection with rAds were seeded in a 96-well tissue culture plate and incubated for 24hours. MTS [3-(4,5-dimethylthiazol-2-yl)-5-(3-carboxymethoxyphenyl)-2-(4-sulfophenyl)-2H-tetrazolium] solution was added and incubated for 2hours, and the absorbance at 490 nm was measured by using an ELISA plate reader (MTP-120; Corona Electric, Ibaragi, Japan).

Animal studies

The following investigations were performed in accordance with the guidelines of our Institutional Animal Care and Use Committee. Six-week-old immunocompetent female BALB/c-jcl mice (CLEA Japan, Tokyo, Japan) were injected subcutaneously on both sides of the flank on day 0 with 3×10^5 MM45T.Li cells infected with each rAd at an in vitro MOI of 5. For the next 5 days (days 1–5), mice received 75 mg/kg of intraperitoneally administered ganciclovir (GCV; Tanabe Pharmaceutical Drug, Tokyo, Japan). In some series of experiment, 1 μg of the recombinant human MCP-1 in 200 μL of PBS containing 1% bovine serum albumin (BSA-PBS) were injected intraperitoneally as previously described (12) from days 0 to 2 (3 consecutive days) in

the group of the tumor cells transduced with Ad-lacZ on HSV-tk/GCV suicide therapy. Tumor sizes were measured every 3 days, and tumor volumes were calculated according to the formula (longest diameter)/ (shortest diameter) ^{2} / 2.

Immunohistochemical analysis

Tumor tissues and spleens were resected on day 10. The tissue samples were embedded in OCT compound (Sakura Finetek, Toorrance, CA, USA) and snap frozen in liquid nitrogen. Cryostat sections of the frozen tissues were fixed with 4% paraformaldehyde (PFA) in PBS, followed by washing once with distilled water for 5 min and 3 times with PBS for 5 min. To avoid nonspecific staining, avidin and biotin in the tissues were blocked by using a blocking kit (Vector Laboratories, Burlingame, CA, USA).

The tissue sections were subsequently stained with rat anti-mouse CD4 Ab, rat anti-mouse CD8a Ab, rat anti-mouse CD11b Ab (BD Biosciences, San Diego, CA, USA), or monoclonal mouse anti-human MCP1 Ab (R&D systems, Minneapolis, MN, USA) overnight at 4°C. Isotype controls were also used. Then, the slides were incubated for 0.5 hours at room temperature with biotinylated polyclonal rabbit anti-rat IgG (Dako Cytomation, Tokyo, Japan), or the antibodies in the M.O.M. immunodetection kit to detect mouse primary antibodies on mouse tissues (Vector Laboratories). The reactions were visualized by using a VectaStain ABC standard kit (Vector Laboratories), followed by counterstaining with hematoxylin. The positive cells were counted in 10 randomly chosen fields at 400-fold magnification by an examiner without any prior knowledge of the experimental procedures.

Quantitative real-time RT-PCR

Total RNA was extracted from tumor tissues resected on day 10 using an RNeasy Mini kit (Qiagen, Hilden, Germany) according to the manufacturer's instructions. After treating the RNA preparations with ribonuclease-free deoxyribonuclease (DNase) I (Qiagen, Hilden, Germany) to remove residual DNA, cDNA was synthesized as described previously (19). Quantitative real-time PCR was performed on a StepOne™ real-time PCR system (Applied Biosystems, Foster City, CA) by using the comparative C_T quantification method. TaqMan® Gene Expression Assays (Applied Biosystems, Foster City, CA) containing specific primers (assay ID: TNF, Mm00443258_m1; GAPDH, Mm99999915_g1), TaqMan® MGB probe (FAM™ dye-labeled), and TaqMan® Fast Universal PCR Master Mix were used with 10 ng cDNA to quantify the expression levels of TNF. Reactions were performed for 20 s at 95°C followed by 40 cycles of 1 s at 95°C and 20 s at 60°C. GAPDH was amplified as an internal control, and the GAPDH C_T values were subtracted from C_T values of the target genes (C_T). The ΔC_T values of tumors after immune gene therapy with both the suicide gene (HSV-tk system) and rAds were compared respectively.

Flow cytometry

MM45T.Li cells transfected with rAds were resuspended in PBS containing 1% BSA and 0.1% sodium azide and incubated for 30 min on ice with PE-conjugated rat anti-human MCP-1 (BD Pharmingen, San Diego, CA). The cells were washed, resuspended in PBS, and analyzed in a FACScan with CellQuest software (FACSCalibur, BD Biosciences, San Jose, CA).

Depletion of macrophages/monocytes

Clodronate liposome was prepared and systemic depletion of monocytes/macrophages was performed as previously described (13, 14). Mice were intraperitoneally injected with 200 μL of clodronate liposome five times: days −2, 0, 3, 6, and 10 after tumor injection. PBS-clodronate was given in the same manner as a negative control. Depletion of CD11c-negative monocytes in blood was confirmed by flow cytometry after injection of clodronate liposome.

Statistical analysis

Mean and SD or SE were calculated for the obtained data. The statistical significance of differences between groups was evaluated by the Mann-Whitney *U* test. $P < 0.05$ was considered statistically significant.

Results

In vitro and in vivo MCP-1 production by cells infected with recombinant adenoviruses.

When various tumor cells were infected with either Ad-mMCP1 or Ad-sMCP1 at a MOI of 10, the cells did not show any signs of cell death (data not shown). Both types of adenoviruses induced the secretion of human MCP-1 into the supernatants to similar levels in all the cell lines that we examined (Fig. 2a). On the contrary, MCP-1 contents in the membrane fractions were higher in the cells infected with Ad-mMCP-1 than in those with Ad-sMCP1 (Fig. 2a). The proportion of MCP-1-positive cells were progressively augmented in MM45T.Li cells as the MOIs of the used Ad-mMCP1 were increased (Fig. 2b). In contract, MCP-1-positive cells were not detected in tumor cells infected with Ad-sMCP1 and Ad-lacZ, even when the cells were infected with either vector at a MOI of 100 (Fig. 2b). Thus, Ad-mMCP1 infection can in vitro drive human MCP-1 expression on the cell surface as well as its secretion into the culture medium. These results indicate that large amounts of MCP-1 protein were expressed and accumulated on the tumor cell surface when tumor cells were infected with Ad-mMCP1 as compared to Ad-sMCP1 in vitro. In order to define the biological functions of secreted human MCP-1 protein, we examined the migratory capacity of splenocytes to the culture supernatants obtained 24 hours after the infection. The supernatants from either Ad-mMCP1- or Ad-sMCP1-infected cells enhanced the transmigration of splenic lymphocytes to similar extents, compared to those from Ad-lacZ-infected cells (Fig. 2c). These results indicated that biologically active human MCP-1 was secreted into the culture supernatants.

Proliferation of tumor cells infected with rAds in vitro and in vivo.

To quantify the proliferation of tumor cells infected with rAds, the MTS assay was performed 24 hours after infection. The optical absorbance at 490 nm of tumor cells did not change in the presence or absence of rAd infection (Fig. 3a). Next, tumor cells infected with rAds (MOI 10) ex vivo were transferred subcutaneously in syngeneic wild-type mice, and tumor development was monitored (Fig. 3b). Tumor cells infected with Ad-mMCP1 and Ad-sMCP1 showed similar growth rates to tumor cells infected with Ad-lacZ. These results indicate that infection with the rAds used in this study did not affect the proliferation of tumor cells in vitro and in vivo and that the delivery of mMCP-1 did not display antitumor activity when used alone. In addition, the levels of MCP-1 expression were confirmed immunohistochemically in the subcutaneous tumor tissues (Fig. 3c). MCP-1-positive tumor cells were detected in tumor tissues infected with Ad-mMCP1, however the cells were negative for MCP-1 staining in tissues infected with Ad-sMCP1 and Ad-lacZ. Moreover, larger amounts of MCP-1 were detected in the tumor tissues of the mice treated with Ad-mMCP1 than in those with Ad-sMCP1 (Fig. 3d). The data indicated that large amounts of MCP-1 protein were expressed and accumulated on the tumor cell surface when the tumor cells were infected with Ad-mMCP1 in vivo.

Potentiation of HSV-tk/GCV suicide therapy by co-infection with Ad-mMCP1.

We previously demonstrated that the gene delivery of Ad-sMCP1 enhanced the antitumor effects of the HSV-tk/GCV system (4-6, 15, 16). Hence, we compared the effects of Ad-mMCP1- and Ad-sMCP1-infection on HSV-tk/GCV suicide therapy. When MM45T.Li cells were co-infected with Ad-tk and Ad-lacZ and received GCV, tumor growth was delayed marginally but not significantly (Fig. 4a). Co-infection with Ad-tk and Ad-sMCP1 retarded tumor growth significantly after GCV treatment. Moreover, tumor growth was almost abrogated by the combination of co-infection with

Ad-tk and Ad-mMCP1 and GCV treatment. To address whether the antitumor effects could be induced not only by the gene delivery using Ad vector but also by the administration of recombinant protein, we gave intraperitoneally recombinant MCP-1 (rMCP-1) to the animals, which were injected with tumor cells, treated with Ad-lacZ and Ad-tk. The systemic administration of rMCP-1 rather enhanced tumor growth (Fig. 4b). Because we previously demonstrated that MCP-1 can promote tumor growth in a context-dependent manner by recruiting macrophages, which can secrete angiogenic factor, vascular endothelial growth factor (VEGF) (15, 17), systemic MCP-1 injection may promote tumor growth by its pro-angiogenic activities.

Recruitment and activation of macrophages and T lymphocytes in tumor tissues.

GCV treatment following co-infection with Ad-lacZ and Ad-tk failed to increase the intratumoral numbers of Mac-1-positive macrophages, CD4-positive lymphocytes, and CD8-positve lymphocytes, compared with GCV treatment following Ad-lacZ infection (Fig. 5a, b). GCV administration following co-infection with Ad-sMCP1 and Ad-tk increased the intratumoral Mac-1-positive macrophage, CD4-positive lymphocyte, and CD8-positve lymphocyte numbers (Fig. 5a, b). The increases were further enhanced by GCV treatment following co-infection with Ad-mMCP1 and Ad-tk (Fig. 5a, b). Moreover, intratumoral mRNA expression of TNF, a known macrophage and T lymphocyte secretagogue, was markedly enhanced in tumors co-infected with Ad-mMCP1, compared with those with Ad-sMCP1 plus Ad-tk. To evaluate the functional contribution of intratumoral immune cells, we depleted CD11c-negative monocytes/macrophages by intraperitoneal administration of clodronate liposome (CL) in the current mouse model. The monocyte/macrophage-depleted mice developed larger tumor than those treated with PBS liposome (Fig. 5d), indicating that monocytes/macrophages were critically

involved in the suppression of tumor growth by Ad-mMCP1. Collectively, these data demonstrate that the delivery of mMCP-1 promoted the recruitment and activation of macrophages and T lymphocytes in tumor tissues, presumably leading to the beneficial antitumor responses in this model.

Discussion

We have proposed a strategy for improving the efficacy of suicide gene-based gene therapy by the combined heterochronic administration of *HSV-tk* and *MCP-1* genes (4-6, 15-17). In the current study, we generated recombinant adenovirus Ad-mMCP1 expressing a fusion protein containing the human MCP-1 cDNA fused with the membrane-spanning domain of fractalkine/CX3CL1, in order to drive more efficient and sessile expression of MCP-1. Ad-mMCP1 infection did not affect the proliferation of MM45T.Li tumor cells in vitro or in vivo, by itself. Of interest is that Ad-mMCP1 infection pontentiated HSV-tk/GCV suicide therapy more efficiently than Ad-sMCP1. Moreover, Ad-mMCP1-mediated antitumor effects were associated with the recruitment and activation of macrophages and T lymphocytes in tumor tissues. Collectively, the delivery of membrane-bound *MCP1* gene can augment antitumor effects caused by the HSV-tk/GCV system in an immunecompetent mouse model of liver tumor and therefore, can be a novel strategy of immune-based gene therapy to prevent tumor proliferation and recurrence in patients with HCC.

Chimeric membrane-bound cytokine gene expression vectors were generated to drive the efficient expression on tumor cell surface and to reduce the severe side effects caused by systemic administration of high doses of cytokines. With this maneuver, cytokines can be anchored on the cell plasma membrane. As a consequence, a locally high concentration of cytokines can be achieved with ease and their in vivo half-life can be prolonged in the tumor site. The availability of cytokines on tumor cell surface can eventually bring immune cells to the tumor site for better antigen uptake and stimulation, thereby inducing antitumor effects at a higher efficiency. Based on these assumptions, this type of modified cytokine gene therapy has been reported on IL-2 (18-20), IL-12 (21), fractalkine (CX3CL1) (22) and TNF (23). Indeed, accumulating evidence revealed

that the membrane-bound form of cytokine genes can exhibit more antitumor effects than the corresponding soluble ones. Likewise, the current study confirms that the membrane-bound form of MCP-1 can attract more immune cells including monocytes/macrophages and T lymphocytes, to the tumor sites and can induce the expression of TNF. In addition, TNF can activate endothelial cells to express several adhesion molecules such as intercellular adhesion molecules (ICAMs), and vascular cell adhesion molecules (VCAMs) (24-27). Circulating immune cells can utilize these adhesion molecules to effectively transmigrate into the tissues in addition to the direct chemotactic activities exerted by MCP-1.

The effects of MCP-1 on tumor growth was controversial; either destructive (28-30) or protective (31, 32) in a context-dependent manner. Likewise, murine colon carcinoma cell expressing MCP-1 failed to metastasize when injected into mice (28) whereas other carcinoma cells showed enhanced metastasis (31). These discrepancies may be explained by the observations reported by Nesbit *et al* (33). They demonstrated that low-level MCP-1 secretion with modest monocyte infiltration resulted in tumor formation, whereas high secretion was associated with massive monocyte/macrophage infiltration into the tumor mass, leading to its destruction within a few days. Thus, systemic MCP-1 administration may not be able to induce massive monocyte/macrophage infiltration into tumor mass and may promote tumor mass as we observed in the present study. Moreover, we previously revealed that suicide therapy can induce tumor cell apoptosis and that apoptotic tumor cells can secrete MCP-1 more efficiently, thereby recruiting a massive number of macrophages and retarding tumor growth (4). Consistently, we further demonstrated that the delivery of an optimal amount of rAd expressing MCP-1 enhanced the antitumor effects of the HSV-tk/GCV system in a model of HCC (15, 17). Infection with Ad-mMCP1 can sustain MCP-1 expression in tumor tissues more efficiently than that with Ad-sMCP1 as evidenced by

an immunohistochemical analysis on the infected tumor tissues. The sustained MCP-1 expression can potentiate suicide gene therapy more efficiently.

The present data suggest that the use of Ad-mMCP1 can be promising, but several problems remain to be solved before the clinical application. First, subcutaneous tumor models of an HCC cell line may not be relevant to HCCs in patients. However, in cases of nonsurgical procedures for HCC treatment in patients, such as percutaneous radiofrequency ablation therapy (34) and transcatheter arterial chemotherapy (35), administration of the current rAd vectors could be easily applied, immediately once the standard nonsurgical procedures to ensure tumor cell killing. Moreover, rAd can elicit its immunogenicity or cytotoxicity when administered in HCC patients, particularly by the use of intraarterial procedures. Actually, the infection of high doses of rAds causes severe unexpected side effects (36). However, the delivery of membrane-bound form of *MCP-1* gene can cause a high and effective concentration at the tumor sites even when it is administered at a relatively lower titer and therefore, can evade severe adverse effects caused frequently by the administration of a high titer of adenovirus vectors.

Acknowledgements

We thank Mariko Katsuda for assistance with histopathological analysis and immunohistochemistry and Maki Kawamura and Chiharu Minami for providing animal care.

Notes

The authors declare no conflict of interest.

References

1. Venook AP. Treatment of hepatocellular carcinoma: too many options? J Clin Oncol.1994; **12**:1323-1334.

2. Trinchet JC, Beaugrand M. Treatment of hepatocellular carcinoma in patients with cirrhosis. J Hepatol.1997; **27**:756-765.

3. Bruix J. Treatment of hepatocellular carcinoma. Hepatology.1997; **25**:259-262.

4. Sakai Y, Kaneko S, Nakamoto Y, Kagaya T, Mukaida N, Kobayashi K. Enhanced anti-tumor effects of herpes simplex virus thymidine kinase/ganciclovir system by codelivering monocyte chemoattractant protein-1 in hepatocellular carcinoma. Cancer Gene Ther.2001; **8**:695-704.

5. Tsuchiyama T, Kaneko S, Nakamoto Y, Sakai Y, Honda M, Mukaida N, et al. Enhanced antitumor effects of a bicistronic adenovirus vector expressing both herpes simplex virus thymidine kinase and monocyte chemoattractant protein-1 against hepatocellular carcinoma. Cancer Gene Ther.2003; **10**:260-269.

6. Kagaya T, Nakamoto Y, Sakai Y, Tsuchiyama T, Yagita H, Mukaida N, et al. Monocyte chemoattractant protein-1 gene delivery enhances antitumor effects of herpes simplex virus thymidine kinase/ganciclovir system in a model of colon cancer. Cancer Gene Ther.2006; **13**:357-366.

7. Freund CT, Sutton MA, Dang T, Contant CF, Rowley D, Lerner SP. Adenovirus-mediated combination suicide and cytokine gene therapy for bladder cancer. Anticancer Res.2000; **20**:1359-1365.

8. Kim YS. Tumor Therapy Applying Membrane-bound Form of Cytokines. Immune Netw.2009; **9**:158-168.

9. Sato Y, Tanaka K, Lee G, Kanegae Y, Sakai Y, Kaneko S, et al. Enhanced and specific gene expression via tissue-specific production of Cre recombinase using

adenovirus vector. Biochem Biophys Res Commun.1998; **244**:455-462.

10. Kanegae Y, Makimura M, Saito I. A simple and efficient method for purification of infectious recombinant adenovirus. Jpn J Med Sci Biol.1994; **47**:157-166.

11. Ko Y, Mukaida N, Panyutich A, Voitenok NN, Matsushima K, Kawai T, et al. A sensitive enzyme-linked immunosorbent assay for human interleukin-8. J Immunol Methods.1992; **149**:227-235.

12. Nakano Y, Kasahara T, Mukaida N, Ko YC, Nakano M, Matsushima K. Protection against lethal bacterial infection in mice by monocyte-chemotactic and -activating factor. Infect Immun.1994; **62**:377-383.

13. Lu P, Li L, Liu G, van Rooijen N, Mukaida N, Zhang X. Opposite roles of CCR2 and CX3CR1 macrophages in alkali-induced corneal neovascularization. Cornea.2009; **28**:562-569.

14. Sadahira Y, Yasuda T, Yoshino T, Manabe T, Takeishi T, Kobayashi Y, et al. Impaired splenic erythropoiesis in phlebotomized mice injected with CL2MDP-liposome: an experimental model for studying the role of stromal macrophages in erythropoiesis. J Leukoc Biol.2000; **68**:464-470.

15. Tsuchiyama T, Nakamoto Y, Sakai Y, Mukaida N, Kaneko S. Optimal amount of monocyte chemoattractant protein-1 enhances antitumor effects of suicide gene therapy against hepatocellular carcinoma by M1 macrophage activation. Cancer Sci.2008; **99**:2075-2082.

16. Tsuchiyama T, Nakamoto Y, Sakai Y, Marukawa Y, Kitahara M, Mukaida N, et al. Prolonged, NK cell-mediated antitumor effects of suicide gene therapy combined with monocyte chemoattractant protein-1 against hepatocellular carcinoma. J Immunol.2007; **178**:574-583.

17. Kakinoki K, Nakamoto Y, Kagaya T, Tsuchiyama T, Sakai Y, Nakahama T, et

al. Prevention of intrahepatic metastasis of liver cancer by suicide gene therapy and chemokine ligand 2/monocyte chemoattractant protein-1 delivery in mice. J Gene Med.2010; **12**:1002-1013.

18. Chang MR, Lee WH, Choi JW, Park SO, Paik SG, Kim YS. Antitumor immunity induced by tumor cells engineered to express a membrane-bound form of IL-2. Exp Mol Med.2005; **37**:240-249.

19. Ji J, Li J, Holmes LM, Burgin KE, Yu X, Wagner TE, et al. Glycoinositol phospholipid-anchored interleukin 2 but not secreted interleukin 2 inhibits melanoma tumor growth in mice. Mol Cancer Ther.2002; **1**:1019-1024.

20. Ji J, Li J, Holmes LM, Burgin KE, Yu X, Wagner TE, et al. Synergistic anti-tumor effect of glycosylphosphatidylinositol-anchored IL-2 and IL-12. J Gene Med.2004; **6**:777-785.

21. Nagarajan S, Selvaraj P. Glycolipid-anchored IL-12 expressed on tumor cell surface induces antitumor immune response. Cancer Res.2002; **62**:2869-2874.

22. Tang L, Hu HD, Hu P, Lan YH, Peng ML, Chen M, et al. Gene therapy with CX3CL1/Fractalkine induces antitumor immunity to regress effectively mouse hepatocellular carcinoma. Gene Ther.2007; **14**:1226-1234.

23. Rieger R, Whitacre D, Cantwell MJ, Prussak C, Kipps TJ. Chimeric form of tumor necrosis factor-alpha has enhanced surface expression and antitumor activity. Cancer Gene Ther.2009; **16**:53-64.

24. Nooijen PT, Eggermont AM, Verbeek MM, Schalkwijk L, Buurman WA, de Waal RM, et al. Transient induction of E-selectin expression following TNF alpha-based isolated limb perfusion in melanoma and sarcoma patients is not tumor specific. J Immunother Emphasis Tumor Immunol.1996; **19**:33-44.

25. Yang L, Froio RM, Sciuto TE, Dvorak AM, Alon R, Luscinskas FW. ICAM-1 regulates neutrophil adhesion and transcellular migration of TNF-alpha-activated

vascular endothelium under flow. Blood.2005; **106**:584-592.

26. Vanhee D, Delneste Y, Lassalle P, Gosset P, Joseph M, Tonnel AB. Modulation of endothelial cell adhesion molecule expression in a situation of chronic inflammatory stimulation. Cell Immunol.1994; **155**:446-456.

27. VandenBerg E, Reid MD, Edwards JD, Davis HW. The role of the cytoskeleton in cellular adhesion molecule expression in tumor necrosis factor-stimulated endothelial cells. J Cell Biochem.2004; **91**:926-937.

28. Huang S, Singh RK, Xie K, Gutman M, Berry KK, Bucana CD, et al. Expression of the JE/MCP-1 gene suppresses metastatic potential in murine colon carcinoma cells. Cancer Immunol Immunother.1994; **39**:231-238.

29. Rollins BJ, Sunday ME. Suppression of tumor formation in vivo by expression of the JE gene in malignant cells. Mol Cell Biol.1991; **11**:3125-3131.

30. Nokihara H, Yanagawa H, Nishioka Y, Yano S, Mukaida N, Matsushima K, et al. Natural killer cell-dependent suppression of systemic spread of human lung adenocarcinoma cells by monocyte chemoattractant protein-1 gene transfection in severe combined immunodeficient mice. Cancer Res.2000; **60**:7002-7007.

31. Nakashima E, Mukaida N, Kubota Y, Kuno K, Yasumoto K, Ichimura F, et al. Human MCAF gene transfer enhances the metastatic capacity of a mouse cachectic adenocarcinoma cell line in vivo. Pharm Res.1995; **12**:1598-1604.

32. Ueno T, Toi M, Saji H, Muta M, Bando H, Kuroi K, et al. Significance of macrophage chemoattractant protein-1 in macrophage recruitment, angiogenesis, and survival in human breast cancer. Clin Cancer Res.2000; **6**:3282-3289.

33. Nesbit M, Schaider H, Miller TH, Herlyn M. Low-level monocyte chemoattractant protein-1 stimulation of monocytes leads to tumor formation in nontumorigenic melanoma cells. J Immunol.2001; **166**:6483-6490.

34. Curley SA. Radiofrequency ablation of malignant liver tumors. Ann Surg

Oncol.2003; 10:338-347.

35. Tung-Ping Poon R, Fan ST, Wong J. Risk factors, prevention, and management of postoperative recurrence after resection of hepatocellular carcinoma. Ann Surg.2000; **232**:10-24.

36. Marshall E. Gene therapy death prompts review of adenovirus vector. Science.1999; **286**:2244-2245.

Figure legends

Figure 1. Construct of rAds.

Under the control of the CMV/IE promoter and the CAG promoter, rAd Ad-mMCP1 (a) expressing human MCP-1 and the membrane-spanning domain of fractalkine/CX3CL1 in sequence, rAd Ad-sMCP1 (b) expressing MCP-1, rAd Ad-lacZ (c) expressing lacZ and rAd Ad-tk (d) expressing HSV-tk. Solid lines indicate the rAd genome. An open triangle below the rAd genome represents a deletion of adenovirus early regions. Arrows show the orientations of the transcription. GpA, rabbit β-globin poly (A) site.

Figure 2. MCP-1 production in tumor cells infected with rAds.

(a) Concentrations of MCP-1 in the membrane fractions and in the media of hepatoma cells (BNL 1NG A.2, BNL 1ME A.7R.1, MM45T.Li and Hepa1-6) and colon cancer cells (colon 26 clone 20) infected with rAds at a MOI of 10 were measured by ELISA. Each value is the mean SD of triplicate experiments. *, $p < 0.05$ when compared to Ad-sMCP1 by the Mann-Whitney's *U* test. (b) Surface expression of MCP-1 on MM45T.Li cells infected with rAds (Ad-mMCP1, Ad-sMCP1 and Ad-lacZ) at the indicated MOIs was assessed by flow cytometry by using PE-conjugated anti-human MCP-1 antibody. Histograms represent MCP-1 staining of tumor cells. Numbers indicate percentages of MCP-1–positive cells. Surface MCP-1–positive cells were detected in 0.08%, 1.2%, 8.1% and 48.0% of MM45T.Li cells infected by Ad-mMCP1 at MOIs of 0.1, 1, 10 and 100, respectively. The results are representative of three independent experiments. (c) The migratory activity of MCP-1 secreted from rAd-infected tumor cells. Mouse splenic lymphocytes were loaded into the upper wells of transwell chambers, and supernatants of tumor cells infected with rAds at a MOI of 10 were added to the lower wells. Cells that migrated through 8-μm pores to the feeder

tray after 4 h incubation were lysed and detected by CyQuant GR dye that exhibits enhanced fluorescence upon binding cellular nucleic acids. Each value is the mean SE of data from three separate migration chambers.

Figure 3. Proliferation of tumor cells infected with rAds in vitro and in vivo.

(a) Tumor cell growth after the infection of indicated rAds in vitro. A total of 5 x 10^5 of MM45T.Li cells were infected with the rAds at a MOI of 10 and incubated for 24 h. The cell numbers were quantitated by MTS assay. The absorbance was determined at 490 nm with a microplate reader. Each value is the mean SD of data from triplicate experiments. (b) Tumor cell growth after infection of indicated rAds in mice. BALB/c mice were subcutaneously injected with 3 x 10^5 MM45T.Li cells infected with the rAds at a MOI of 10 on day 0. Tumor diameters were monitored. Each value is the mean SE. (c) Immunohistochemical analysis of subcutaneous tumor tissues 7 days after the injection in b. Tissues were stained and visualized by using anti-human MCP-1 Ab and ABC methods. MCP-1 expression was seen as brown in the cytoplasm of tumor cells. The bar represents 30 μm. Original magnification, x 400. (d) Concentrations of MCP-1 were measured in the s.c. tumor tissues resected on day 1 after injection of 5 x 10^6 MM45T.Li cells infected with the indicated rAds at a MOI of 50 by ELISA. Each value is the mean SD of duplicate experiments. *, $p < 0.05$ when compared to Ad-sMCP1 by the Mann-Whitney's *U* test.

Figure 4. Antitumor effects of rAds in vivo.

(a) BALB/c mice were subcutaneously injected with 3×10^5 MM45T.Li cells infected with rAds Ad-mMCP1+Ad-tk, Ad-sMCP1+Ad-tk, Ad-lacZ+Ad-tk, and Ad-lacZ at a MOI of 10 on day 0. Subsequently, 75 mg/kg of GCV was administered for five consecutive days (days 2–6). Each value is the mean SE of triplicate experiments. *, *p*

<0.05 when compared to Ad-sMCP1+Ad-tk and **, *p* <0.01 when compared to Ad-lacZ+Ad-tk by the Mann-Whitney's *U* test. (b) BALB/c mice were injected with MM45T.Li cells and treated as described in the legend to Fig 4a. In Ad-lacZ + Ad-tk + recombinant human MCP-1 (rMCP-1) group, the mice were injected with 1 μg of rMCP-1 intraperitoneally from days 0 to 2 (3 consecutive days). The mice were injected with PBS as controls. Tumor sizes were measured every 3 days. Each value is the mean SE. **, *p* <0.01 when compared to Ad-lacZ+Ad-tk+rMCP-1 by the Mann-Whitney's *U* test.

Figure 5. Immunohistochemical analysis for Mac-1-, CD4- and CD8a-positive cells and expression of TNF mRNA in tumor tissues.

In the experiment described in the legend to Figure 4, tumors were resected on day 10 and used for the analyses. (a) Tumor tissues treated with Ad-mMCP1+Ad-tk (a, e and i), Ad-sMCP1+Ad-tk (b, f and j), Ad-lacZ+Ad-tk (c, g and k) and Ad-lacZ (d, h and l) were stained with anti-Mac-1 antibody (a - d), anti-CD4 antibody (e - h) or anti-CD8a antibody (i - l). Positive cells are seen as brown. Original magnification, x 400. (b) Quantitative morphometric analysis showing the proportions of positive cells in areas of 100 tumor cells. Ten high-power (x400) fields of tumor tissue were examined. Results are expressed as means per 1000 hepatoma cells. Values are the means SD of triplicate experiments. *, *p* <0.05 when compared to Ad-sMCP1 by the Mann-Whitney's *U* test. (c) Real-time PCR analysis for TNF mRNA expression in tumor tissues, presented relative to GAPDH mRNA. Each value is the mean SD of duplicate experiments. *, *p* <0.05 when compared to Ad-sMCP-1+Ad-tk by the Mann-Whitney *U* test. (d) BALB/c mice were subcutaneously injected with MM45T.Li cells infected with indicated rAds and treated as described in the legend to Fig. 4a. In the Ad-mMCP-1 + Ad-tk + clodronate liposome (CL) group, mice were injected with 200 μL of CL to deplete

monocytes/macrophages as described in Materials and Methods. The mice were injected with PBS liposome (PBS) as controls. Tumor sizes were measured every 3 days. Each value is the mean SE. *, p <0.05 when compared to Ad-mMCP-1+Ad-tk+PBS by the Mann-Whitney U test.

Figure 1

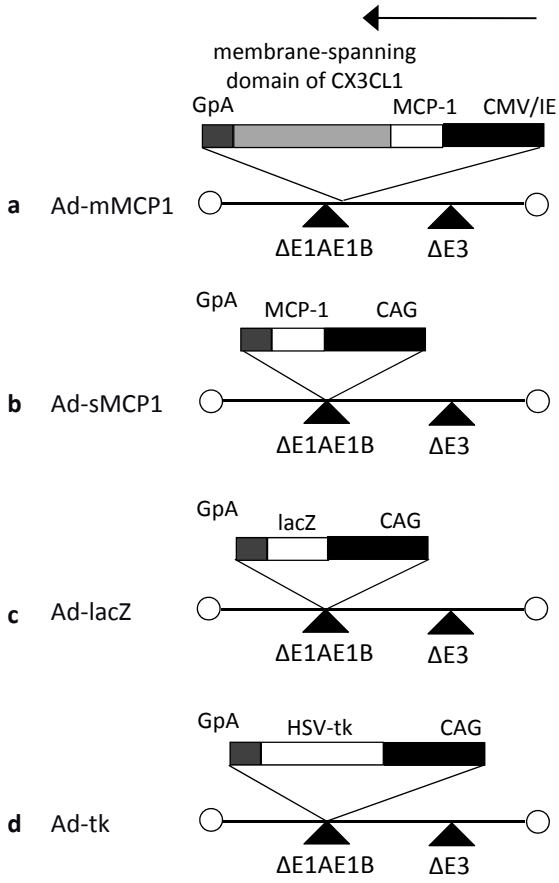
membrane-spanning
domain of CX3CL1
GpA
MCP-1
CMV/IE
a
Ad-mMCP1
ΔE1AE1B
ΔE3
GpA
MCP-1
CAG
b
Ad-sMCP1
ΔE1AE1B
ΔE3
GpA
lacZ
CAG
c
Ad-lacZ
ΔE1AE1B
ΔE3
GpA
HSV-tk
CAG
d
Ad-tk
ΔE1AE1B
ΔE3

Figure 2

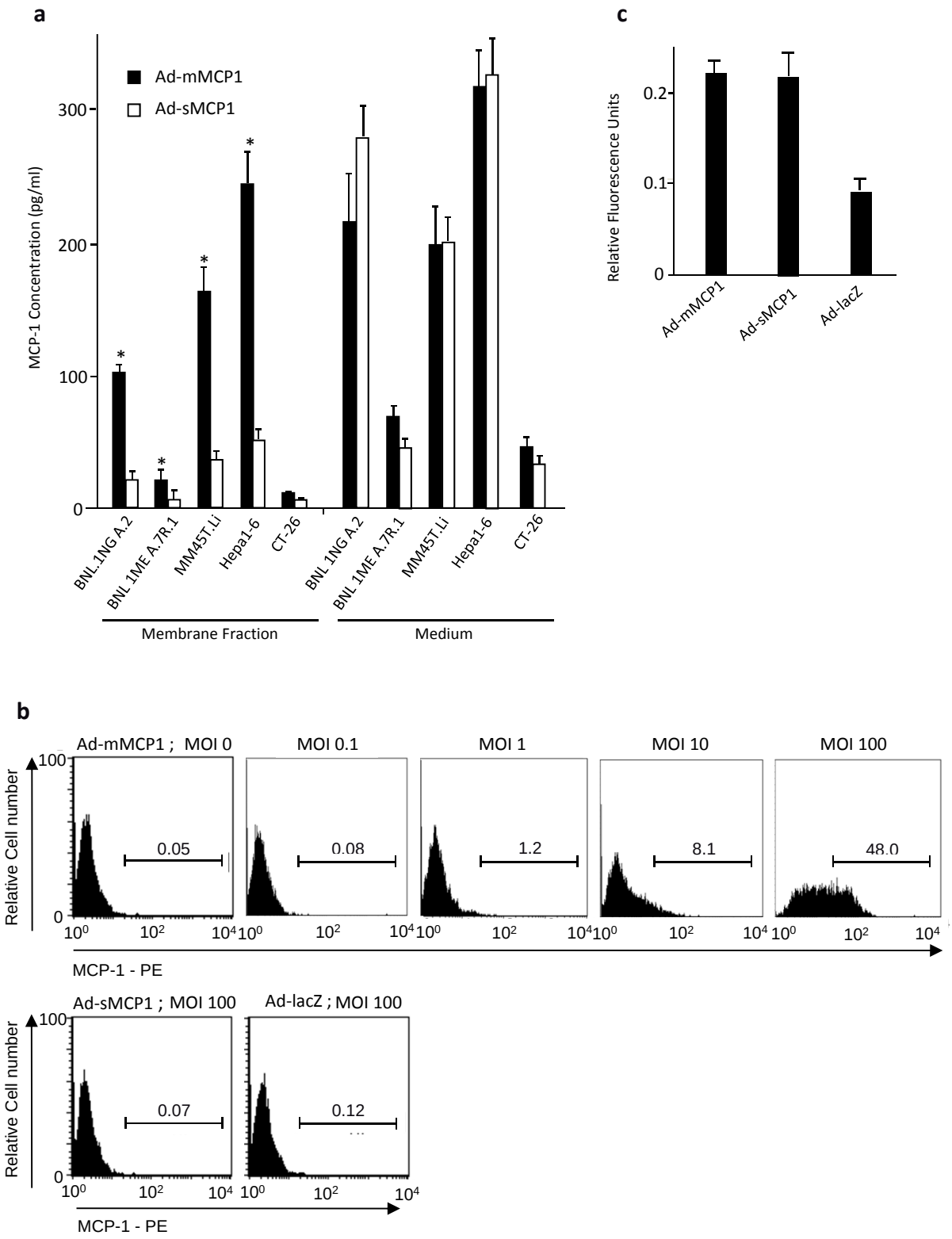
a
Ad-mMCP1
Ad-sMCP1
MCP-1 Concentration (pg/ml)
300
200
100
0
*
BNL.1NG A.2
BNL.1ME A.7R.1
MM45T.Li
Hepa1-6
CT-26
Membrane Fraction
Medium
c
Relative Fluorescence Units
0.2
0.1
0
Ad-mMCP1
Ad-sMCP1
Ad-lacZ
b
Ad-mMCP1 ; MOI 0
MOI 0.1
MOI 1
MOI 10
MOI 100
Relative Cell number
100
0
0.05
0.08
1.2
8.1
48.0
10^0
10^2
10^4
MCP-1 - PE
Ad-sMCP1 ; MOI 100
Ad-lacZ ; MOI 100
0.07
0.12

Figure 3

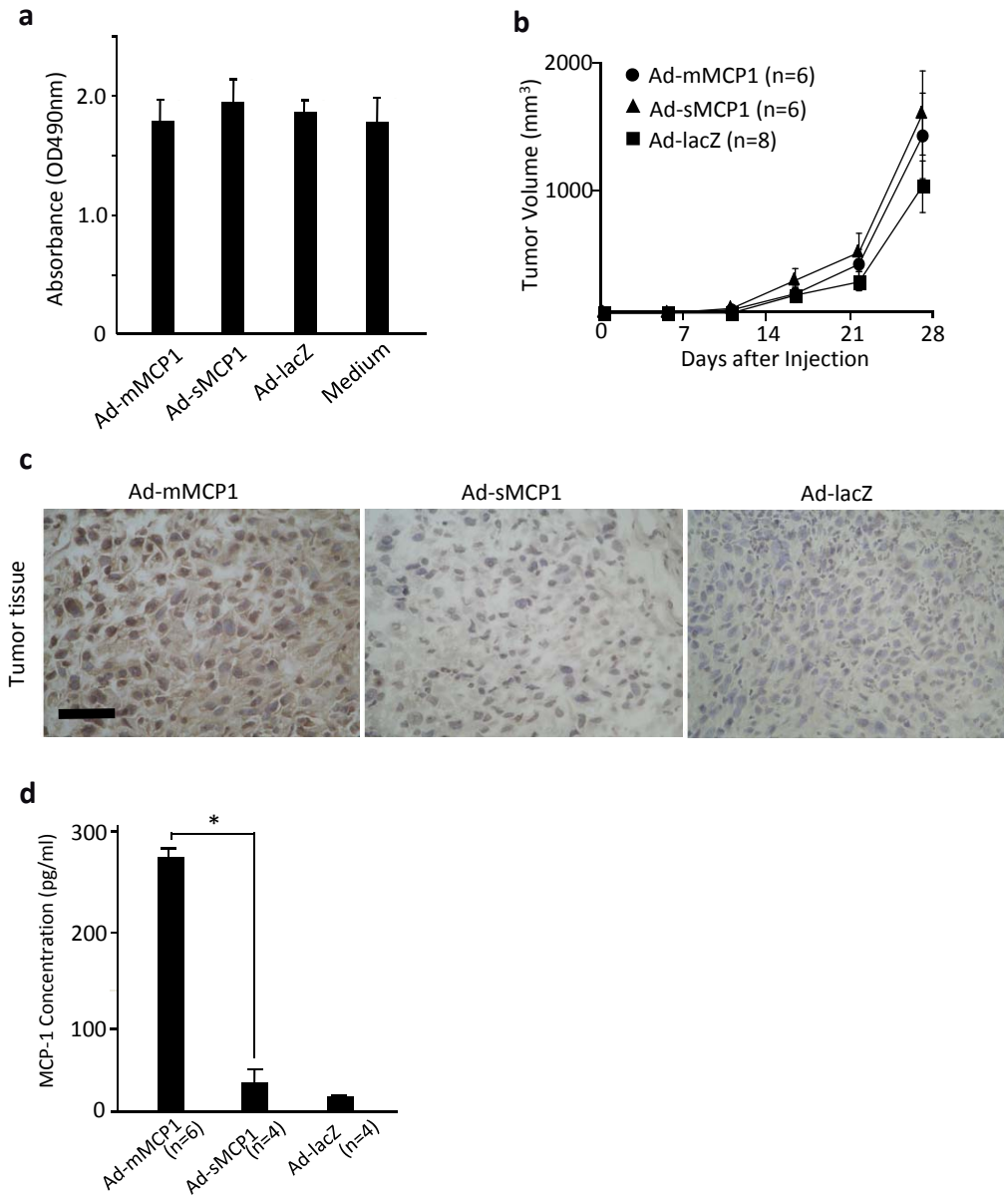
a
Absorbance (OD490nm)
2.0
1.0
0
Ad-mMCP1
Ad-sMCP1
Ad-lacZ
Medium
b
Tumor Volume (mm3)
2000
1000
Ad-mMCP1 (n=6)
Ad-sMCP1 (n=6)
Ad-lacZ (n=8)
0
7
14
21
28
Days after Injection
c
Ad-mMCP1
Ad-sMCP1
Ad-lacZ
Tumor tissue
d
MCP-1 Concentration (pg/ml)
300
200
100
0
*
Ad-mMCP1 (n=6)
Ad-sMCP1 (n=4)
Ad-lacZ (n=4)

Figure 4

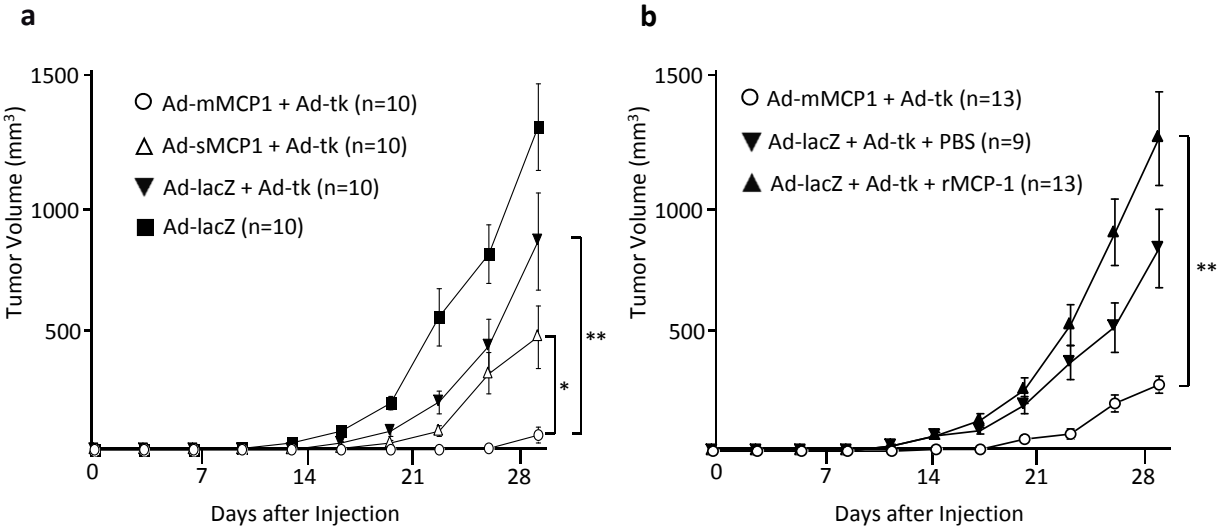
a
1500
1000
500
Tumor Volume (mm3)
Ad-mMCP1 + Ad-tk (n=10)
Ad-sMCP1 + Ad-tk (n=10)
Ad-lacZ + Ad-tk (n=10)
Ad-lacZ (n=10)
**
*
0
7
14
21
28
Days after Injection
b
1500
1000
500
Tumor Volume (mm3)
Ad-mMCP1 + Ad-tk (n=13)
Ad-lacZ + Ad-tk + PBS (n=9)
Ad-lacZ + Ad-tk + rMCP-1 (n=13)
**
0
7
14
21
28
Days after Injection

Figure 5

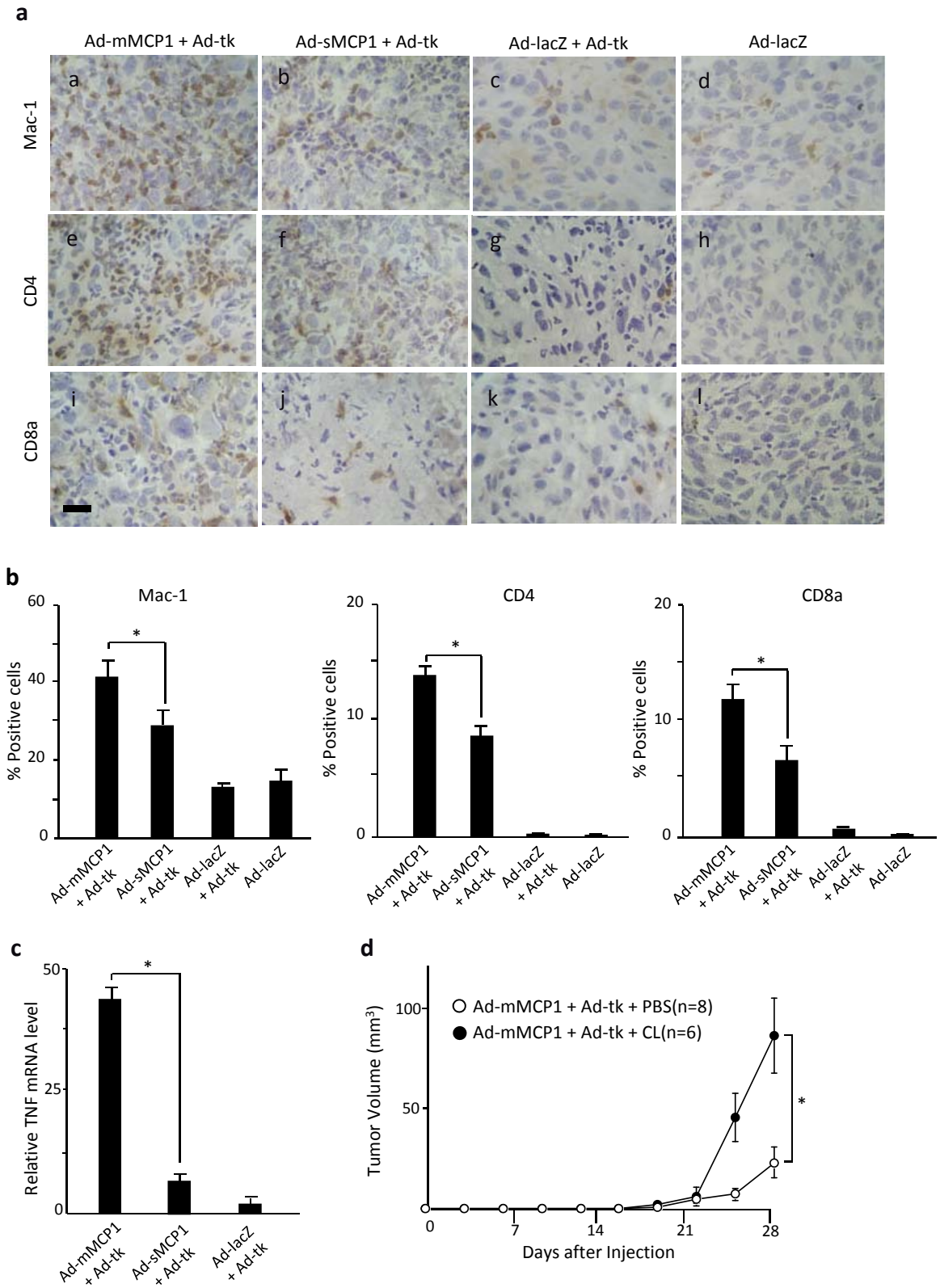
a
Ad-mMCP1 + Ad-tk
Ad-sMCP1 + Ad-tk
Ad-lacZ + Ad-tk
Ad-lacZ
Mac-1
CD4
CD8a
b
Mac-1
CD4
CD8a
% Positive cells
Ad-mMCP1 + Ad-tk
Ad-sMCP1 + Ad-tk
Ad-lacZ + Ad-tk
Ad-lacZ
c
Relative TNF mRNA level
d
Ad-mMCP1 + Ad-tk + PBS(n=8)
Ad-mMCP1 + Ad-tk + CL(n=6)
Tumor Volume (mm3)
Days after Injection